ORIGINAL RESEARCH PAPER

Adsorption Behaviors of Curcumin on N-doped TiO_2 Anatase Nanoparticles: Density Functional Theory Calculations

Amirali Abbasi [1, 2, 3]*, ***Jaber Jahanbin Sardroodi*** [1, 2, 3]

[1] *Molecular Simulation Laboratory (MSL), Azarbaijan Shahid Madani University, Tabriz, Iran*
[2] *Computational Nanomaterials Research Group (CNRG), Azarbaijan Shahid Madani University, Tabriz, Iran*
[3] *Department of Chemistry, Faculty of Basic Sciences, Azarbaijan Shahid Madani University, Tabriz, Iran*

Received: 2017-04-29 Accepted: 2017-05-20 Published: 2017-06-25

ABSTRACT

The density functional theory (DFT) calculations were used to get information concerning the interaction of curcumin with pristine and N-doped TiO_2 anatase nanoparticles. Three adsorption geometries of curcumin over the TiO_2 anatase nanoparticles were studied in order to fully exploit the sensing properties of TiO_2 nanoparticles. Curcumin molecule adsorbs on the fivefold coordinated titanium sites of the TiO_2 nanoparticle because of the high affinity of these sites with respect to the curcumin molecule. A preferred perpendicular adsorption of curcumin on the OC-substituted nanoparticle was found to be the most favorable conformation with the estimated adsorption energy of about -5.33 eV. The results suggest that the curcumin molecule favorably interacts with the N-doped TiO_2 nanoparticle, that is, the interaction of curcumin with the pristine nanoparticle is less favorable in energy than the interaction with the N-doped one. The structural parameters such as bond lengths/angles and adsorption energies were examined in the discussion of results. The electronic structures of the system were analyzed in view of the density of states and molecular orbitals. The analysis of projected density of states and molecular orbitals showed forming new chemical bonds between the nanoparticle and curcumin molecule. By including vdW interactions, the adsorption energies of the most stable curcumin+TiO_2 couples were increased, implying the dominant effect of dispersion energy.

Keywords: *: Density functional theory; TiO_2 nanoparticle; Curcumin; Adsorption, Molecular orbital*

How to cite this article
Abbasi A, Jahanbin Sardroodi J. Adsorption Behaviors of Curcumin on The N-Doped TiO_2 Anatase Nanoparticles Using density Functional Theory Calculations. J. Nanoanalysis., 2017; 4(1): 85-98. DOI: 10.22034/jna.2017.01.010

INTRODUCTION

Titanium dioxide (or Titania) is a semiconducting metal oxide, which has excellent physical and chemical properties (e.g., high activity, outstanding stability, non-toxicity and low-cost) [1-3]. TiO_2 can be seen in an extensive range of technological applications such as photocatalysis, heterogeneous catalysis, dye-sensitized solar cells and gas sensor devices [3-6]. Three important crystalline polymorphs of TiO_2 have been known as named by rutile, anatase, and brookite. Among three polymorphs of TiO_2, rutile and anatase have given eminent importance since they play a key role in the potential applications of TiO_2 [7]. Rutile

* Corresponding Author Email: a_abbasi@azaruniv.edu, Tel: +98 (041)24327500

is thermodynamically the most stable polymorph of Titania, and it can withstand high temperatures, while anatase and brookite polymorphs subject to a transformation when heated. The electronegativity of the oxygen atom of TiO_2 is much higher than that of titanium atom, which makes that the shared electrons to be located over the oxygen atom. As a result, the titanium atom has a positive charge, whereas the oxygen atom turns out to be negatively charged. In the case of nanoparticles, the anatase phase has more activity than the rutile and brookite ones and is more energetically favorable structure. This has been observed experimentally for example, in the case of the TiO_2 thin layers [8]. During the last decades, the study of the adsorption and sensing properties of TiO_2 has attracted substantial attentions [9-12]. We reported the results of DFT computations on the interactive behaviors of curcumin with the pristine and N-doped TiO_2 nanoparticles. The main concern associated with TiO_2 is its wide band gap (3.2 eV), which significantly limits the photocatalytic activity of TiO_2. [13-15]. It has been well understood that the band gap of TiO_2 should be tuned by different methods. [15-18]. One of the most appropriate methods is replacing the oxygen atom of TiO_2 by a suitable nonmetal element such as nitrogen (nitrogen doping), which acceptably improves the optical sensitivity of TiO_2 [19-23]. Recently, numerous computational studies of the adsorption of different air pollutants on the TiO_2 have been published. For example, Tang et al. Reported the insights of DFT calculations of the adsorption of nitrogen oxides on graphene, graphene oxides and Pd-decorated graphene oxides [24, 25]. Also, theoretical investigations on the adsorption of ammonia and nitrogen dioxide on TiO_2/MoS_2 and TiO_2/Gold nanocomposites have been carried out in our previous works [26, 27]. On the experimental point of view, several studies have regarded synthesis of mesoporous TiO_2–curcumin nanoparticles, functionalization of TiO_2 nanoparticles and curcumin loading for enhancement of biological activity, photo-degradation of curcumin in the presence of TiO_2 nanoparticles and curcumin-sensitized TiO_2 for enhanced photodegradation of dyes under visible light [28-31]. We have used DFT calculations to investigate the molecular adsorption of curcumin on N-doped TiO_2 anatase nanoparticles. The results indicate that the binding of curcumin is stronger on the N-doped nanoparticle than on pristine (undoped) one. Thus, the N-doped nanoparticle has stronger adsorption ability than the undoped one for curcumin detection. An important aim in our research is to study methods to improve the interaction of curcumin with modified N-doped TiO_2 anatase nanoparticles. It is well demonstrated that nitrogen doping is conductive to the interaction of a curcumin molecule with TiO_2 nanoparticles.

COMPUTATIONAL METHODS AND MODELS OF NANOPARTICLES

Details of DFT calculations

All DFT calculations [32, 33] were performed using the Open source Package for Material explorer (OPENMX3.8) package using an energy cutoff of 150 Ry [34, 35]. This package utilizes pseudo-atomic orbitals (PAOs) as basis sets to expand a one-particle Kohn-Sham (KS) wave functions [35]. The considered PAOs were set to be 3s-3p-1d for the titanium atom, 2s-2p for the oxygen, nitrogen and carbon atoms and 1s for the hydrogen atom within the cutoff radii of 7 for the titanium and 5 for the oxygen, nitrogen, carbon and hydrogen atoms. The generalized gradient approximation (GGA) utilizing the Perdew-Burke-Ernzerhof (PBE) exchange and correlation functionals were used in all energy calculations [36]. Energy convergence was set to be 10^{-4} Hartree/Bohr, while for the self-consistent field (SCF) iterations, the convergence criterion of 10^{-6} Hartree was used. For visualization of adsorption configurations and molecular orbitals presented in this study, XCrysDen program was used [37]. In the present work, the dispersion correction was analyzed using Grimme's DFT-D2 approach, which corrects the adsorption energies for the dispersion energy [38]. The D2 correction method was included in the calculations by an appropriate keyword. By including this correction, the effects of vdW interactions were taken into account in our calculations. Since OpenMX uses localized orbitals as basis function, it is very important to take account of basis set superposition error (BSSE) when we investigate an effect of a weak interaction such as vdW interaction. However, the employment of BSSE depends strongly on the type of "EigenvalueSolver" in the input file. The empty atom scheme enables us to estimate the basis set superposition error (BSSE) using the counterpoise correction (CP) method. We have set the "cluster" method as "Eigenvalue Solver" in our calculations. In the case of cluster method, there is not necessary

to calculate BSSE factor. The optimized structure of curcumin molecule was represented in Figure 1.

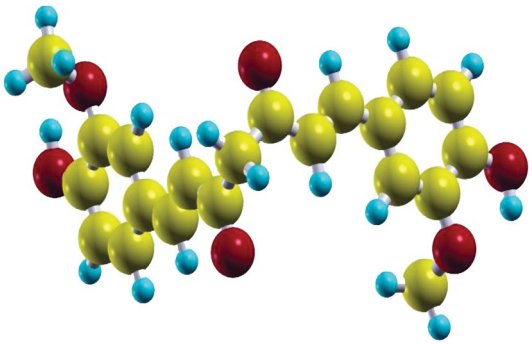

Fig. 1. Schematic presentation of a curcumin molecule.

The adsorption energy was predicted using the following formula:

$\Delta E_{ads} = E$ [particle + adsorbate] – (E [particle] + E [adsorbate])

where E [particle + adsorbate], E [particle] and E [adsorbate] are the total electronic energies of the complex system (TiO_2 + Curcumin), bare TiO_2 particle and Curcumin molecule, respectively. According to this formula, the more negative the adsorption energy, the more energy favorable the adsorption configuration.

Models of nanoparticles

The 72 atoms TiO_2 anatase nanoparticle was constructed through putting 3×2×1 numbers of TiO_2 unit cells along x, y and z axis, respectively. The dimension of the simulation box is 20 Å ×15 Å ×30 Å, which is much higher than the size of the particle. The repeated particles were separated by a large vacuum region of 11.5 A˚ to avoid the interactions between repeated layers. The unit cell was taken from "American Mineralogists Database" webpage [39], reported by Wyckoff [40]. Figure 2 displays the optimized geometry of the TiO2 anatase nanoparticle. Labels O_C, O_T and O_D in this figure indicate the "threefold coordinated oxygen ", "twofold coordinated oxygen", and "dangling oxygen" atoms, respectively. The crystal structure of TiO_2 anatase contains two types of titanium atoms, namely fivefold coordinated titanium (5f-Ti) and sixfold coordinated titanium (6f-Ti) and two types of oxygen atoms, namely threefold coordinated oxygen (3f-O) and twofold coordinated oxygen (2f-O) atoms [41, 42]. 3f-O and 2f-O atoms were replaced by nitrogen atoms in order to model N-doped nanoparticles. The reactivities of 5f-Ti and 2f-O are much higher than those of 6f-Ti and 3f-O. The N-doped TiO_2 anatase nanoparticles were geometrically optimized as shown in Figure 3. Since the adsorption of a curcumin molecule on N-doped nanoparticles is stronger than the adsorption on undoped ones, N-doped particles can react with curcumin molecule more efficiently, compared with the undoped ones. Therefore, the N-doped particles have higher sensing capability than the undoped ones due to their higher adsorption energies. Besides this, there are more adsorption sites on the N-doped particles because of their higher activities in the adsorption process, on which the adsorption energies are more negative than those of the undoped nanoparticles. It implies that N doped particles are more active and they can interact with curcumin molecule strongly. So, the nitrogen doping method acts as an efficient method to adsorb curcumin and other molecules through the surface adsorption strategy, that is, the nitrogen doping is conductive to the interaction of TiO_2 with curcumin molecule [12, 20].

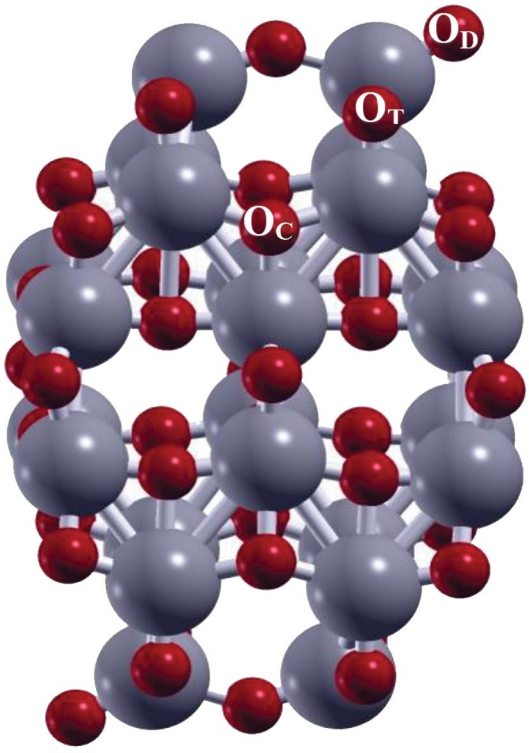

Fig. 2. Optimized geometry of an undoped TiO_2 anatase nanoparticle constructed from the 3×2×1 unit cells. Labels O_C, O_T and O_D indicate threefold coordinated (central oxygen), twofold coordinated oxygen and dangling oxygen atoms, respectively.

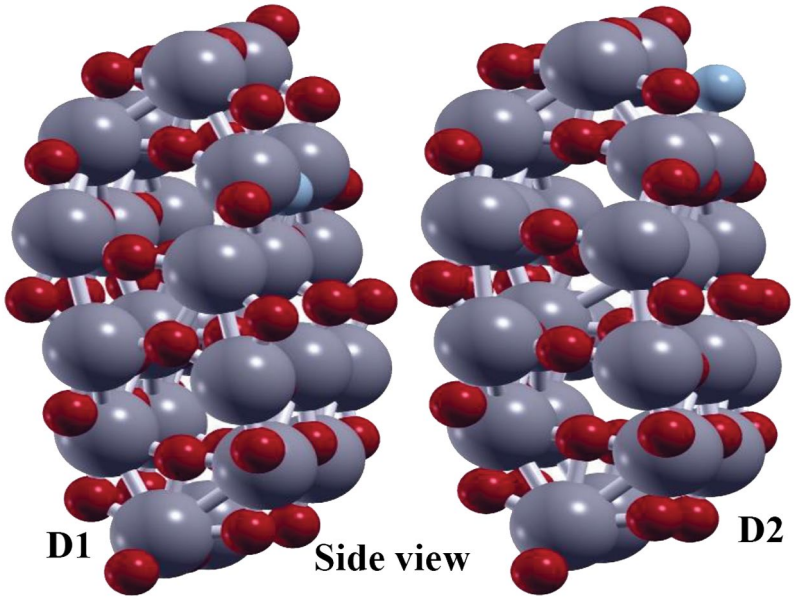

Fig. 3. Optimized N-doped TiO_2 anatase nanoparticles constructed from the 3×2×1 unit cells; (D1) O_C-substituted nanoparticle. (D2) O_T-substituted one.

RESULT AND DISCUSSION

Bond lengths, angles and adsorption energies

For curcumin adsorption on the undoped and N-doped TiO_2 nanoparticles, three adsorption sites were analyzed and considered as the most stable adsorption configurations. The adsorption configurations of curcumin on the fivefold coordinated titanium atoms were depicted in Figure 4 (configurations A and B).

Figure 5 displays the adsorption configuration for undoped particle adsorption system (configuration C).

These figures show the optimized configurations of curcumin molecule adsorbed to the Ti site of undoped and N-doped nanoparticles. In configuration A, curcumin molecule interacts with the O_C-substituted TiO_2 nanoparticle, while configuration B represents the interaction of curcumin with O_T-substituted nanoparticle. These configurations provide a single contacting point between curcumin and TiO_2 nanoparticle and the binding site was located on the fivefold coordinated titanium atom. Table 1 lists the lengths for the newly formed Ti-O bonds between the titanium atom of TiO_2 and the oxygen atom of curcumin molecule.

These configurations are known as perpendicular configurations because of the vertical position of curcumin towards the nanoparticle. Adsorption energy analysis was conducted in this work in order to entirely examine the interaction of curcumin with considered TiO_2 nanoparticles. Table 1 lists the adsorption energies calculated using different methods. The adsorption energy of curcumin on the O_C-substituted nanoparticle (configuration A) is higher (more negative) than that of the O_T-substituted nanoparticle (configuration B), indicating that the adsorption of curcumin on the O_C-substituted nanoparticle is energetically more favorable than the adsorption on the O_T-substituted one. Therefore, for this type of adsorption, the configurations with O_C-substituted nanoparticle are the most stable configurations. Moreover, adsorptions on the N-doped nanoparticles (configurations A and B) are found to be more favorable in energy than the adsorption on the undoped one (configuration C). Of the three configurations, configuration A has the highest adsorption energy (-5.33 eV), making it the most likely biding site to be located in the O_C-substituted nanoparticle. Since the N-doped nanoparticles have higher adsorption energy than the undoped ones, it can be concluded that the nitrogen doping strengthens the adsorption of curcumin on the TiO_2. In other words, doping of nitrogen atom is conductive to the adsorption of curcumin on the nanoparticle. Based on the obtained results, we found that the nitrogen doping is an efficient method in order to fully improve the adsorption ability of pristine TiO_2 nanoparticles. It means that the N-doped nanoparticles have the stronger sensing capability than the pristine ones.

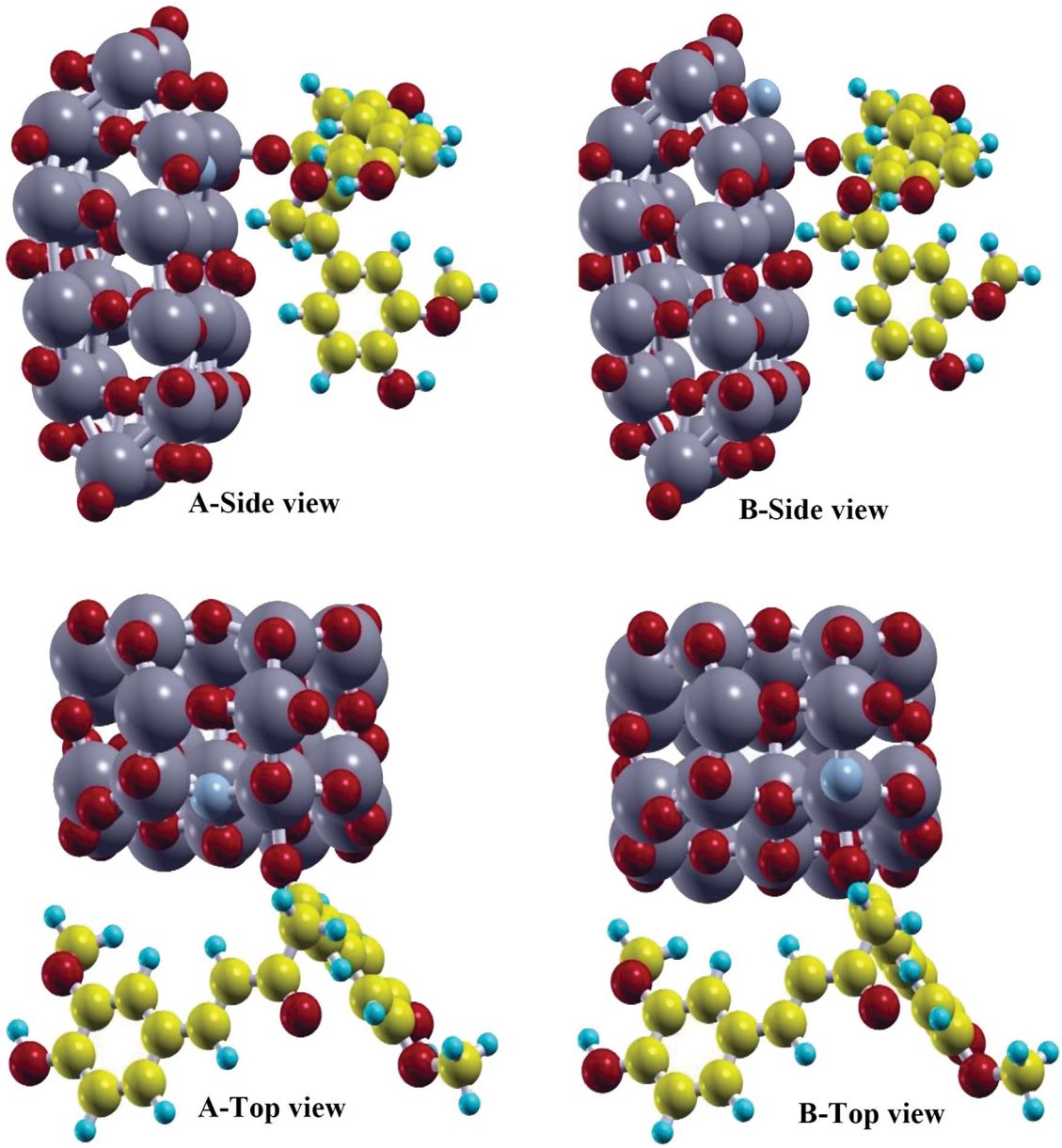

Fig. 4. Optimized geometry configurations of curcumin molecule adsorbed onto the N-doped TiO_2 anatase nanoparticles. Colors represent atoms accordingly: Ti in gray, O in red, N in blue, C in yellow and H in cyan.

Table 1. Calculated bond lengths and distances (in Å), adsorption energies (in eV) and charge transfers of curcumin molecule adsorbed on the fivefold coordinated titanium sites of undoped and N-doped TiO_2 anatase nanoparticles

Configuration	Newly formed Ti-O	Adsorption energy		Mulliken charge
		PBE	DFT-D2	
A	2.13	-5.33	-12.22	-1.03
B	2.14	-5.24	-11.98	-1.06
C	2.02	-1.98	-8.83	-0.48

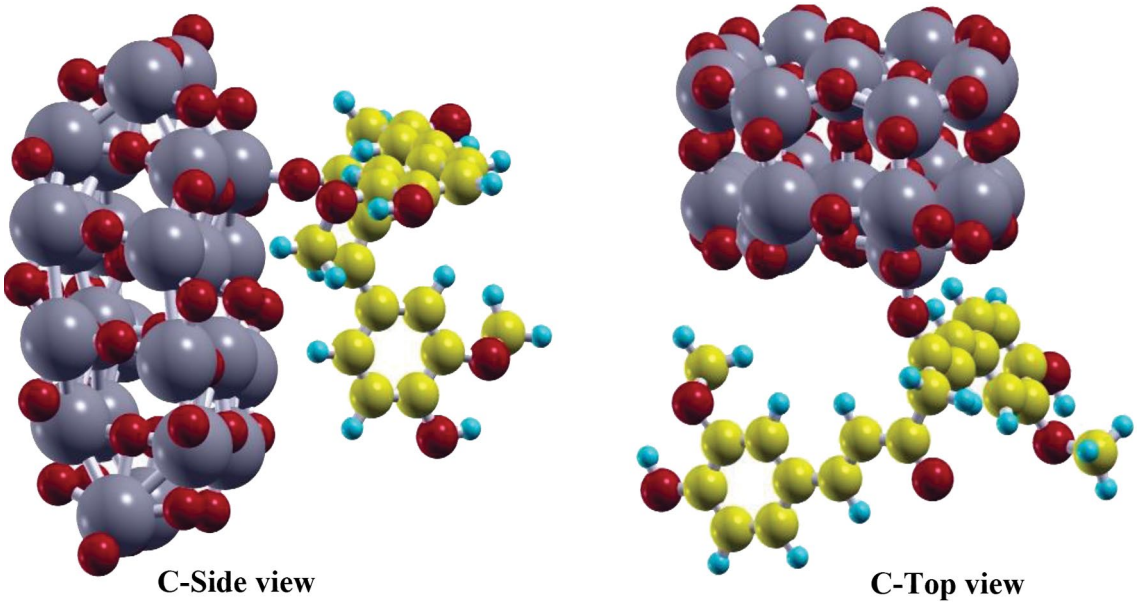

Fig. 5. Optimized geometry configurations of curcumin molecule adsorbed onto the undoped TiO_2 anatase nanoparticles. Colors represent atoms accordingly: Ti in gray, O in red, N in blue, C in yellow and H in cyan.

Density of states (DOSs) and Molecular orbitals (MOs)

Figure 6 represents the total density of states (TDOSs) for curcumin adsorption on the fivefold coordinated titanium sites of undoped and N-doped TiO_2 anatase nanoparticles. This Figure displays that the changes between the DOSs of N-doped and undoped TiO_2 are enlarged by adsorption of curcumin. These differences include some main changes in the energies of the peaks, as well as the creation of small peaks in the DOS spectra. Figure 7 presents the projected density of states (PDOSs) for curcumin adsorption on the fivefold coordinated titanium sites of TiO_2 nanoparticles. Panels (a, b) in this figure represent the PDOSs of the titanium atom of TiO_2 and the oxygen atom of curcumin (configurations A and B). The substantial overlaps between the PDOSs of the titanium and oxygen atoms indicate the mutual interaction between them and consequently forming chemical Ti-O bond. Panel (c) represents the relevant PDOSs for configuration C. The large overlaps in these PDOSs also suggest that the titanium atom of the nanoparticle forms a chemical bond with the oxygen atom of curcumin.

Thus, from the PDOS overlaps in the given spectra, we found that the oxygen atom of the curcumin molecule coordinates of the titanium atom of the TiO_2. Figure 8 displays the PDOSs of the titanium atom of nanoparticle and different orbitals of the oxygen atom of curcumin molecule. The higher overlaps between the PDOSs of the titanium and p^1 orbital of the oxygen reveal the higher mutual interaction between them.

Similarly, the PDOSs of the different orbitals of the titanium atom and the oxygen atom of curcumin molecule were represented in Figure 9. It can be seen from this figure that the d^1 orbital of the titanium has a higher overlap and consequently higher interaction with the oxygen atom of the curcumin molecule.

In Figure 10, we can see the highest overlap between the PDOSs of the oxygen atom of the curcumin and d^1 orbital of the titanium atom for configuration C.

These considerable overlaps between the PDOSs of the interacting atoms are representative of the high mutual interactions between them. This feature could be a helpful in the development of efficient adsorbents for curcumin molecule. Unfortunately, there exist no detailed experimental data about the adsorption of curcumin molecule on TiO_2 nanoparticle so far.

Figure 11 shows the highest occupied molecular orbital (HOMO) and the lowest unoccupied molecular orbital (LUMO) of the free curcumin molecule. It can be seen from this figure that the HOMO is strongly localized between the six member rings, whereas the electronic density in the LUMO seems to be distributed over the entire curcumin molecule. In the LUMO molecular orbital, we can see an extensive electronic density distribution over the curcumin molecule.

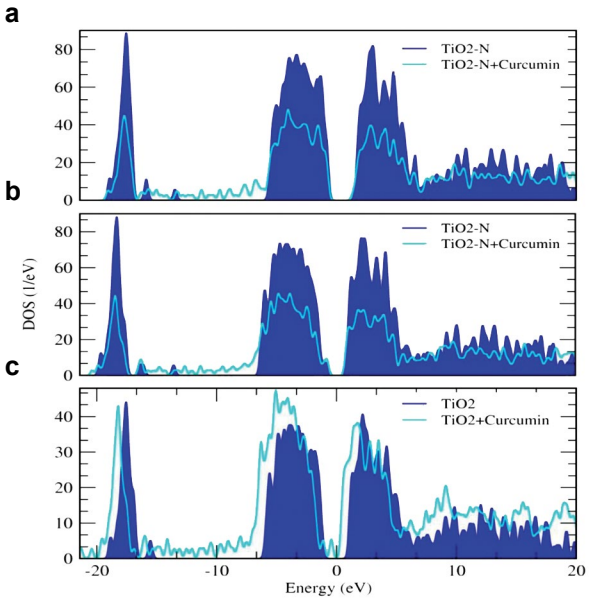

Fig. 6. Total density of states for curcumin molecule adsorbed on the TiO_2 anatase nanoparticles, (a) configuration A, (b) configuration B and (c) configuration C.

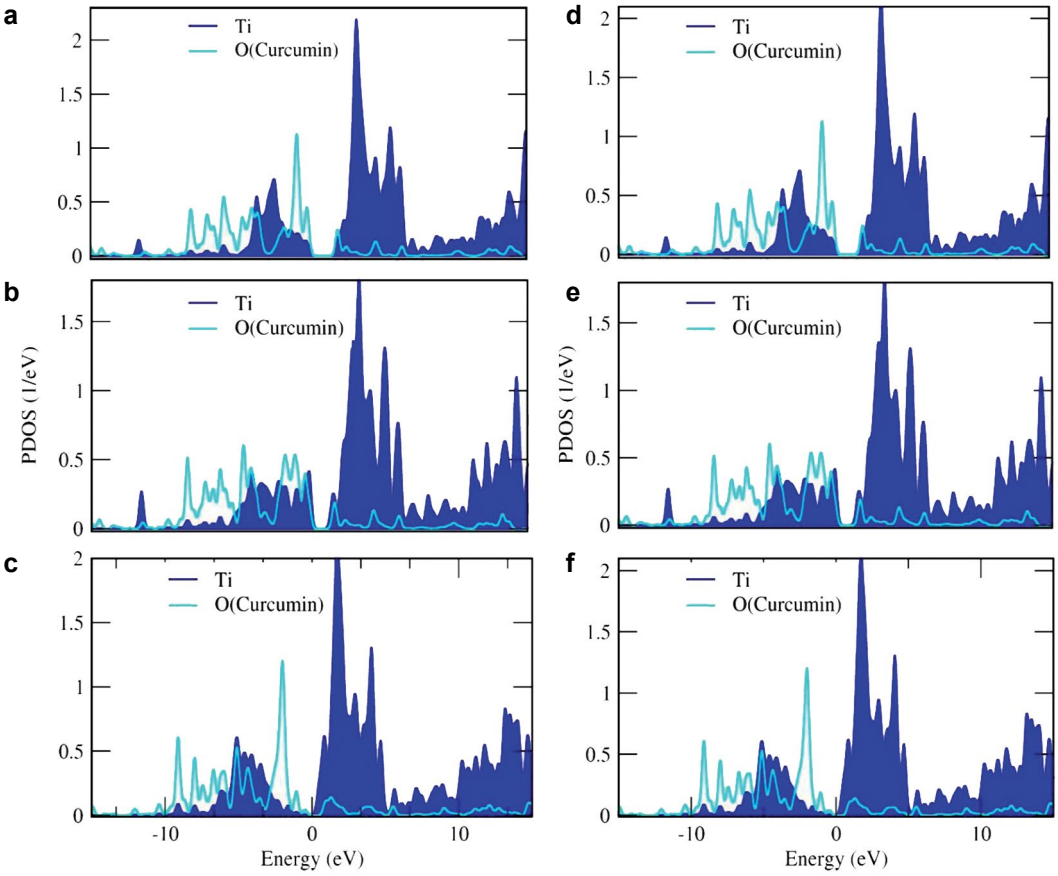

Fig. 7. Projected density of states of curcumin molecule adsorbed on the fivefold coordinated titanium sites of TiO_2 anatase nanoparticles. (a): Configuration A, (b): Configuration B, (c): Configuration C. Panels (a-c) represent the PDOSs obtained from PBE calculations, while panels (d-f) display the PDOSs of DFT-D calculations.

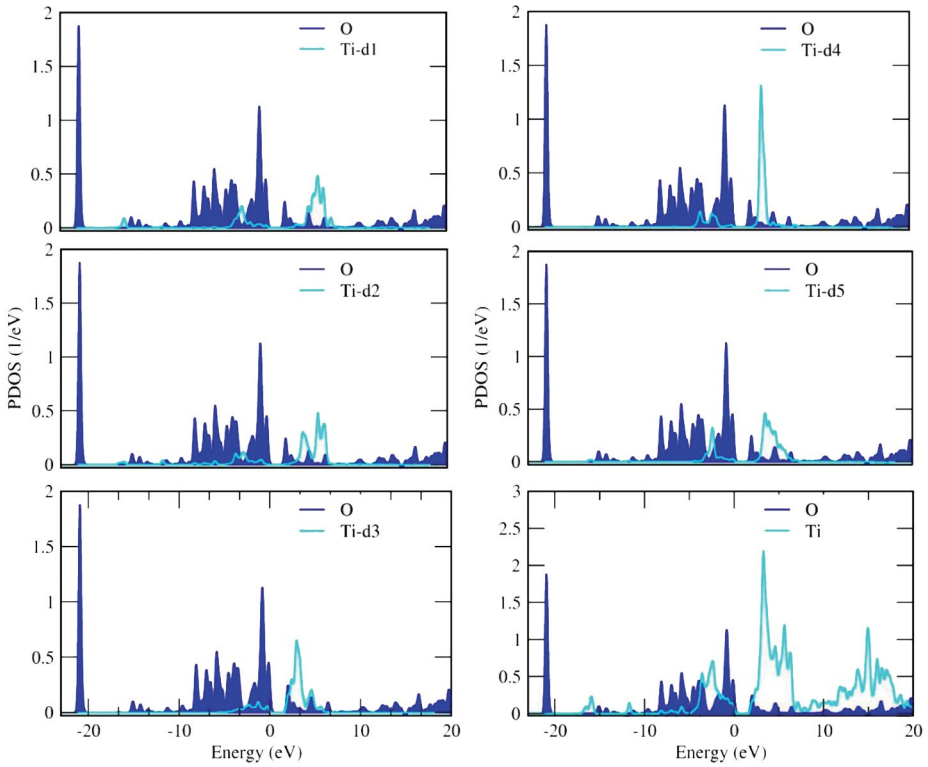

Fig. 8. PDOSs of the oxygen, titanium and different orbitals of the titanium atom for configuration A.

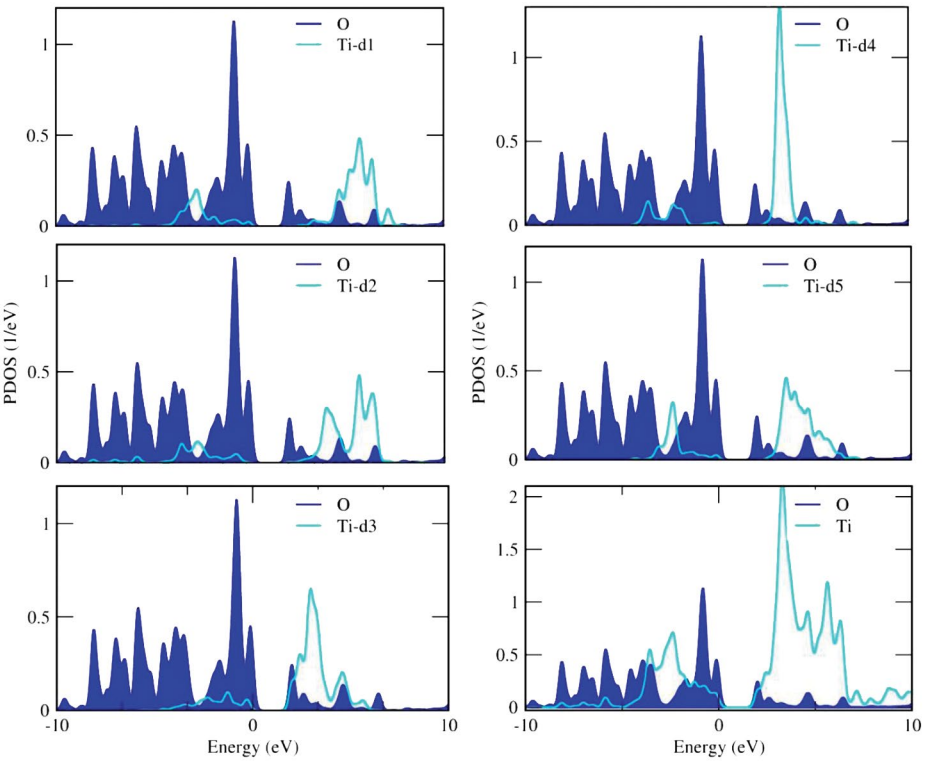

Fig. 9. PDOSs of the oxygen, titanium and different orbitals of the titanium atom for configuration B.

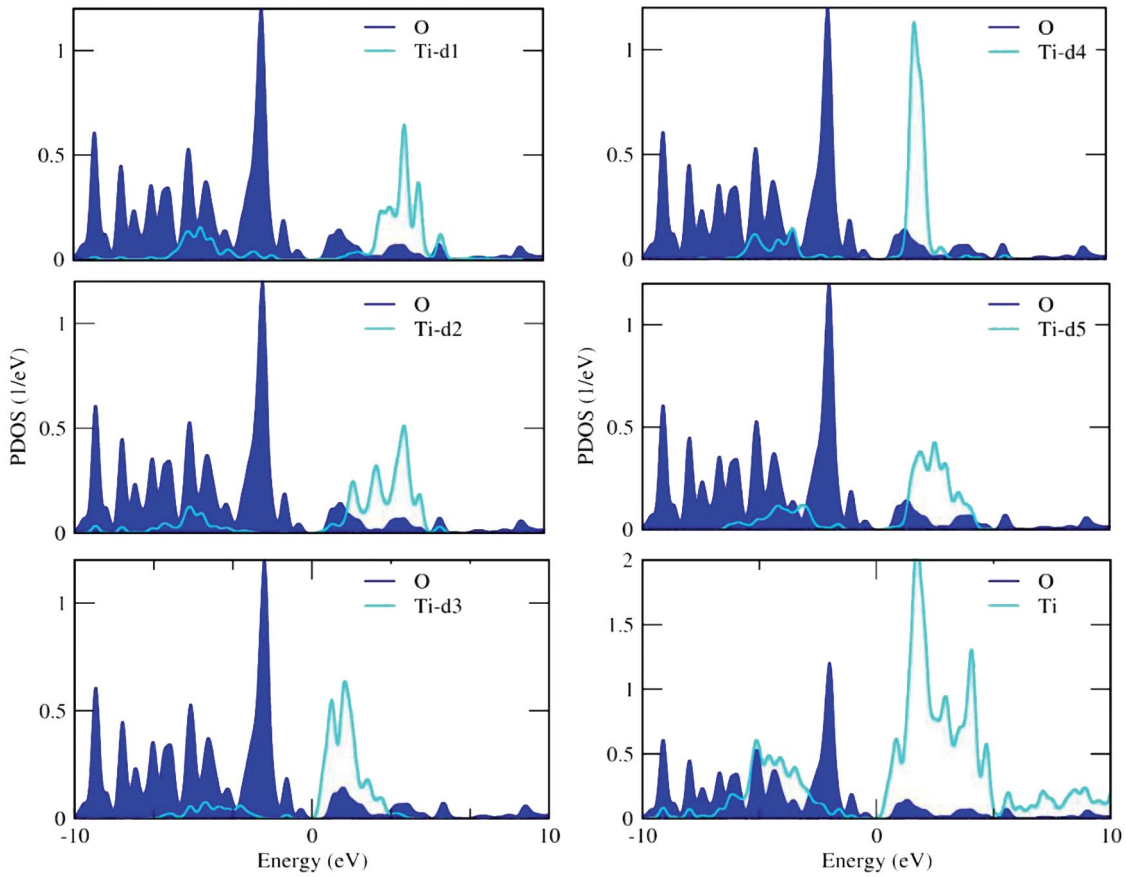

Fig. 10. PDOSs of the oxygen, titanium and different orbitals of the titanium atom for configuration C.

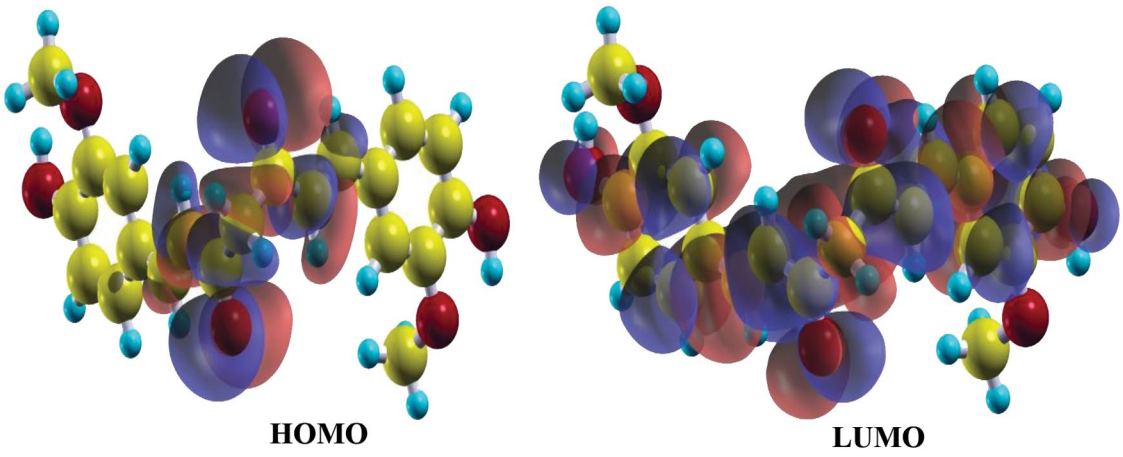

Fig. 11. HOMO-LUMO molecular orbitals for non-adsorbed curcumin molecule.

Figures 12 and 13 represent the isosurfaces of HOMO and LUMO molecular orbitals of TiO_2 nanoparticles with adsorbed curcumin molecules (configurations A and B). As distinct from these figures, the electronic densities in the HOMOs and LUMOs were largely spread on the curcumin molecule rather than TiO_2 nanoparticle.

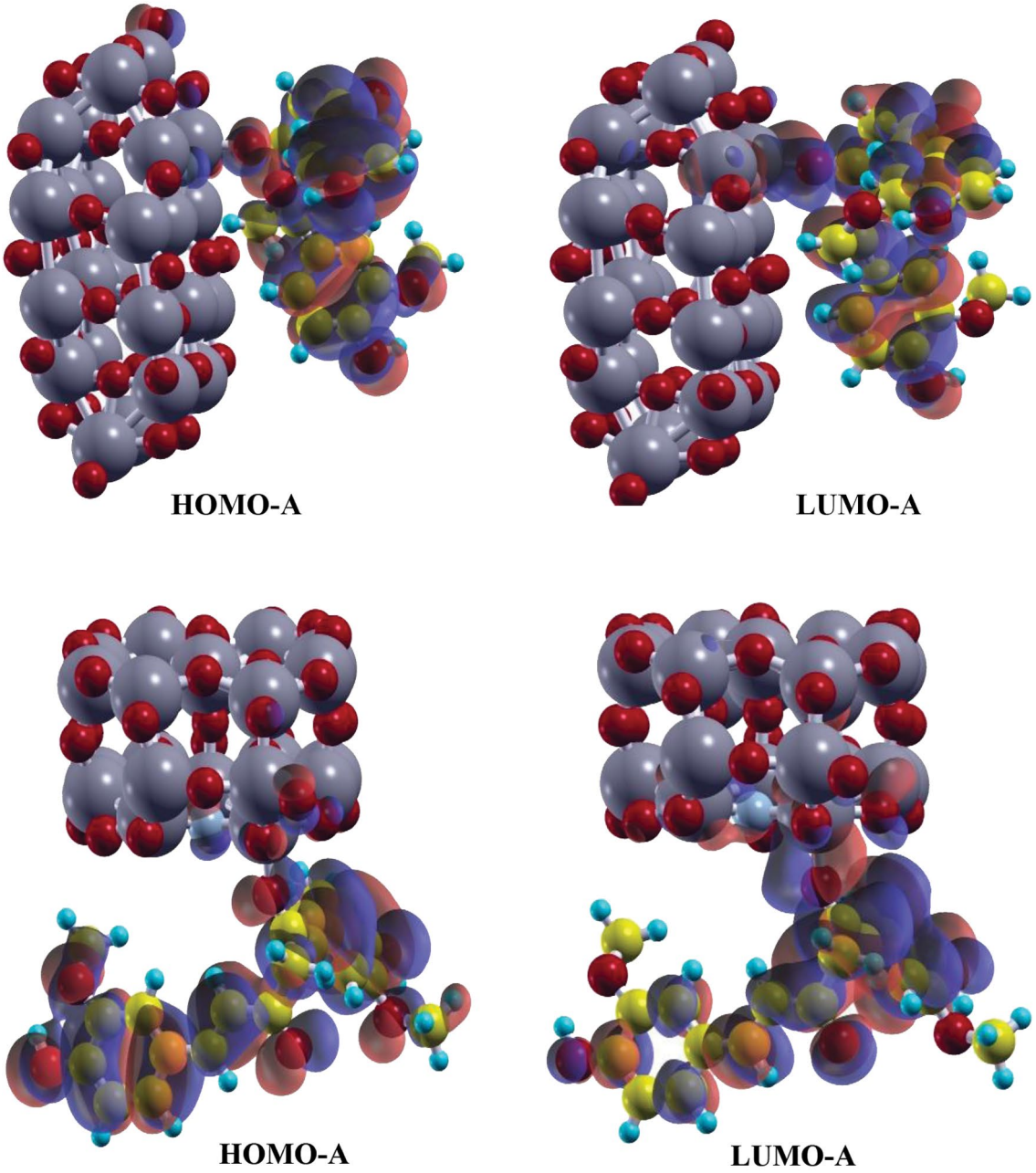

Fig. 12. Side and top views of isosurfaces of HOMO and LUMO molecular orbitals for curcumin molecule adsorbed on the TiO_2 anatase nanoparticles (configuration A).

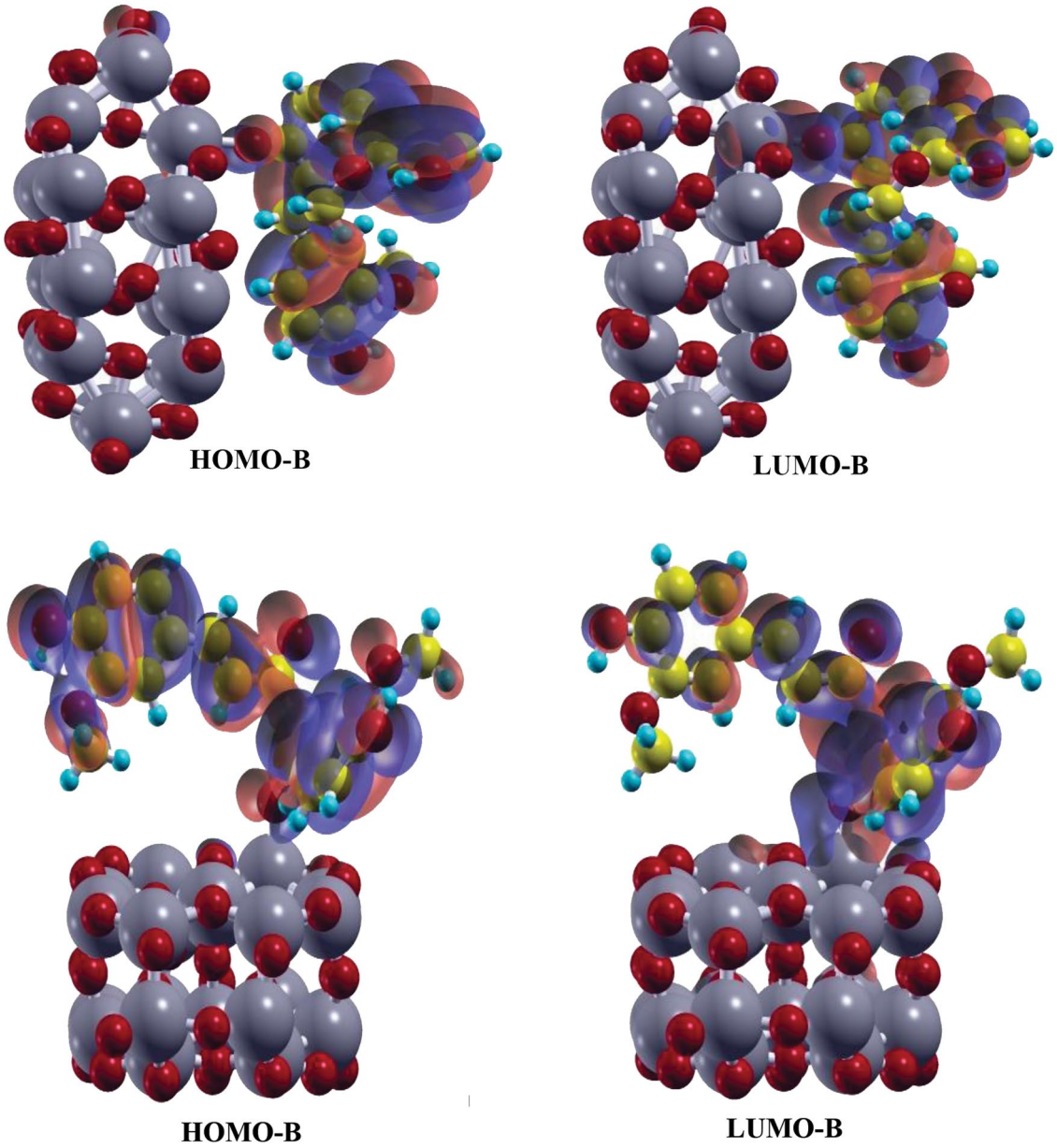

Fig. 13. Side and top views of isosurfaces of HOMO and LUMO molecular orbitals for curcumin molecule adsorbed on the TiO_2 anatase nanoparticles (configuration B).

Figure 14 shows the corresponding HOMO and LUMO isosurfaces for configuration C (undoped particle adsorption system), which displays that the HOMOs are dominant at the curcumin molecule, whereas the electronic densities in the LUMOs seem to be distributed on the TiO_2 nanoparticles.

Figure 15 displays the differences of the electronic densities for curcumin molecule adsorbed on the TiO_2 anatase nanoparticles, representing the distribution of electronic densities over the whole nanoparticle with adsorbed curcumin molecule. However, these variations in the electronic structure of the studied nanoparticle would affect the electronic transport properties of the nanoparticles and this feature can provide an efficient outline toward improving the sensing capabilities of N-doped TiO_2 nanoparticles for curcumin recognition.

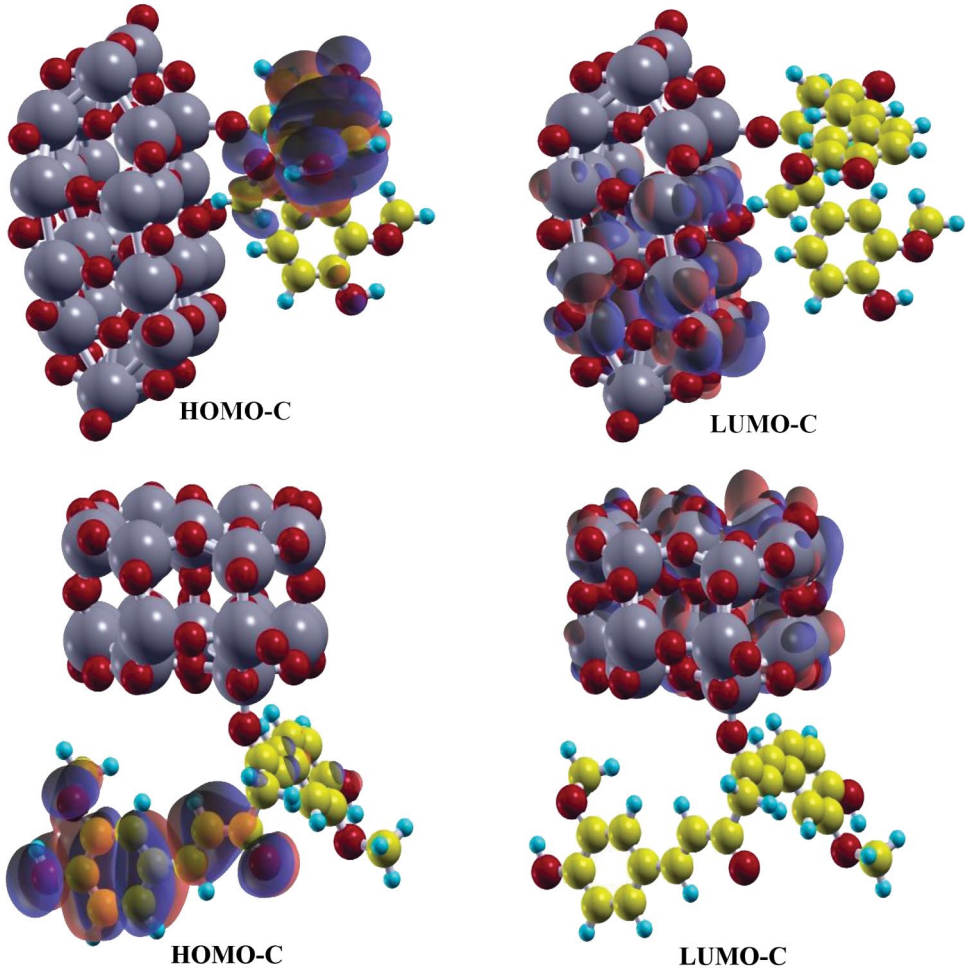

Fig. 14. Side and top views of isosurfaces of HOMO and LUMO molecular orbitals for curcumin molecule adsorbed on the TiO_2 anatase nanoparticles (configuration C).

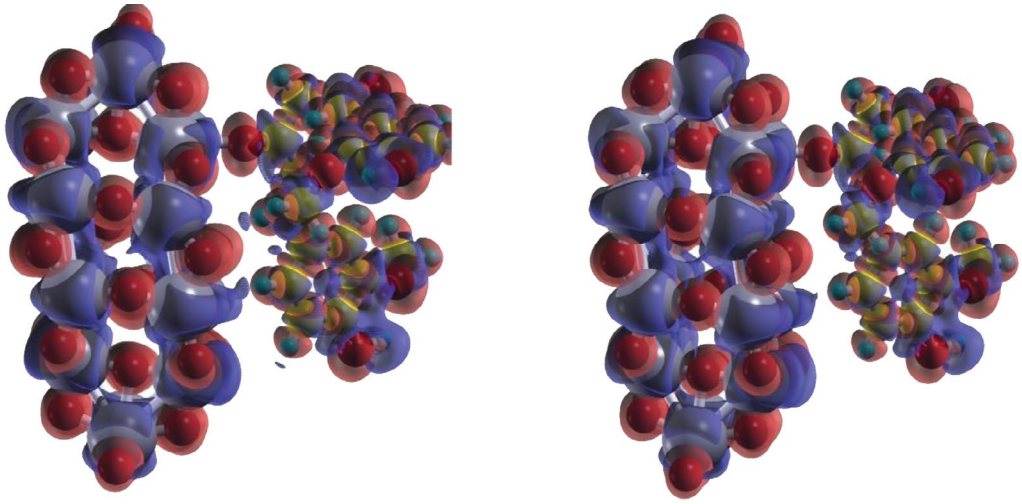

Fig. 15. Differences of the electronic densities for curcumin molecule adsorbed on the TiO_2 anatase nanoparticles.

The charge exchange between the adsorbed curcumin and the TiO_2 nanoparticle

In order to completely analyze the charge transfer between the curcumin and TiO_2 nanoparticles, Mulliken charge analysis was conducted in this work and the results were listed in Table 1. The charge difference for the particle i after and before adsorption, was calculated using the following equation:

$$\Delta Q_i = Q_{i\ (in\ complex)} - Q_{i\ (in\ vacuum)}) \quad (2)$$

where Q_i is the value of the Mulliken charge of the i. Subscript " i " symbolizes the TiO_2 nanoparticle or curcumin molecule. The charge difference, ΔQ, is an amount of the charge shifted to, or, from the studied nanoparticles from, or, to the curcumin molecule. For configuration A, the charge estimation results in a considerable charge transfer of about -1.03 e from curcumin molecule to the nanoparticle, which indicates that curcumin behaves as an electron donor.

CONCLUSION

We have examined the adsorption of curcumin on the pristine and N-doped TiO_2 anatase nanoparticles using the first principles calculations based on the DFT approach. It was found that the adsorption of curcumin molecule on the N-doped nanoparticle is more favorable in energy than the adsorption of curcumin on the undoped one. Thus, N-doped nanoparticles have higher sensing capability than the undoped ones. On the basis of the obtained results, we found that the nitrogen doping is an efficient method in order to fully improve the adsorption ability of pristine TiO_2 nanoparticles. Adsorption on the fivefold coordinated titanium site is found to be more favorable than the adsorption on the other sites. The TDOS of the system represents that the variations between the DOSs of N-doped and pristine TiO^2 are increased by the adsorption of curcumin molecule. We can see some main changes in the energies of the peaks and creation of small peaks. The large overlaps in the PDOS spectra of the interacting atoms confirms well the formation of new bonds between the nanoparticle and adsorbate. It can be seen from the PDOSs of the different orbitals of titanium atom and oxygen atom of curcumin that the d^1 orbital of the titanium has a higher overlap with the oxygen atom of curcumin molecule. Molecular orbitals of the studied systems indicate that the HOMOs and LUMOs were mainly located on the curcumin molecule. The differences of the electronic densities for curcumin adsorbed on the TiO_2 nanoparticles indicate the distribution of electronic densities over the whole TiO_2+curcumin system. The charge analysis based on Mulliken charges reveals a noticeable charge transfer from the adsorbate to the TiO_2 nanoparticle. Therefore, it was suggested that N-doped TiO_2 nanoparticle is an appropriate adsorbent for detection of curcumin molecule and the results provide a theoretical basis to develop effective TiO_2-based sensors for monitoring curcumin molecule.

ACKNOWLEDGMENT

This work has been supported by Azarbaijan Shahid Madani University.

CONFLICT OF INTEREST

The authors declare that there is no conflict of interests regarding the publication of this manuscript.

REFERENCES

1. M.R. Hoffmann, S.T. Matin, W. Choi and D.W. Bahnemann, J. Chem. Rev., 95, 69 (1995).
2. K. Shankar, J.I. Basham, N.K. Allam, O.K. Varghese, G.K. Mor and X. Feng, Phys. Chem. C., 113, 6327 (2009).
3. U. Diebold, Surf. Sci. Reports, 48, 53 (2003).
4. A. Fujishima, X. Zhang and D.A. Tryk, Surf. Sci. Reports, 63, 515 (2008).
5. F. Han, V.S.R. Kambala, M. Srinivasan, D. Rajarathnam and R. Naidu, Applied Catalysis A: General, 359, 25 (2009).
6. A. Abbasi and J.J. Sardroodi, Int. J. Bio-Inorg. Hybr. Nanomater., 5, 43 (2016).
7. M.M. Rodriguez, X. Peng, L. Liu, Y. Li and J.M. Andino, Phys. Chem. C., 116(37), 19755 (2012).
8. M.L. Caariainen, T.O. Kaariainen and D.C. Cameron, Thin Solid Films, 517, 6666 (2009).
9. R. Erdogan, O. Ozbek and I. Onal, Surf. Sci., 604, 1029 (2010).
10. H. Liu, M. Zhao, Y. Lei, C. Pan and W. Xiao, Comput. Mat. Sci., 15, 389 (2012).
11. R. Hummatov, O. Gulseren, E. Ozensoy, D. Toffol and H. Ustunel, Phys. Chem. 116, 6191(2012).
12. J. Liu, Q. Liu, P. Fang, C. Pan and W. Xiao, Appl. Surf. Sci., 258, 8312 (2012).
13. W.J. Yin, S. Chen, J.H. Yang, X.G. Gong, Y. Yan and S.H. Wei, Appl. Phys. Letts., 96, 221901 (2010).
14. S. Livraghi, M.C. Paganini, E. Giamello, A. Selloni, C.D. Valentin and G. Pacchioni, J. Am. Chem. Soc., 128, 15666 (2006).
15. H. Gao, J. Zhou, D. Dai and Y. Qu, J. Chem. Eng. Technol.,

32, 867 (2009).

16. H. Irie, Y. Watanabe, and K. Hashimoto, Phys. Chem. B., 107(23), 5483 (2003).
17. Q. Chen, C. Tang and G. Zheng, Physica B: Condens. Matter, 404, 1074 (2009).
18. A. Abbasi and J. J. Sardroodi, Int. J. Nano Dimens., 7, 349, (2016).
19. I.A. Guzei, A.G. Baboul, G.P.A. Yap, A.L. Rheingold, H.B. Schlegel and C.H. Winter. J. Am. Chem. Soc., 119, 3387 (1997).
20. J. Liu, L. Dong, W. Guo, T. Liang and W. Lai, Phys. Chem. C., 117, 13037 (2013).
21. A. Abbasi and J. J. Sardroodi, J. Water Environ. Nanotechnol., 2, 52 (2017).
22. R. Liu, X. Zhou, F. Yang and Y. Yu, Appl. Surf. Sci., 319, 50 (2014).
23. Z. Zhao and Q. Liu, J. Phys. D: Appl. Phys., 41, 085417 (2008).
24. S. Tang and Z. Cao, J. Chem. Phys., 134, 044710 (2011).
25. S. Tang and J. Zhu, RSC Adv., 4, 23084 (2014).
26. A. Abbasi and J.J. Sardroodi, Int. J. Bio-Inorg. Hybr. Nanomater., 5, 105 (2016).
27. A. Abbasi, J.J. Sardroodi and A. R. Ebrahimzadeh, J. Water Environ. Nanotechnol., 1, 55 (2016).
28. Z.M. Abou-Gamra and M.A. Ahmed, Journal of Photochemistry and Photobiology B: Biology, 160, 134 (2016).
29. V.J. Sawant and R.V. Kupwade, Der Pharmacia Lettre, 7, 37 (2015).
30. U. Singh, S. Verma, H.N. Ghosh, M.C. Rath, K.I. Priyadarsini, A. Sharma, K.K. Pushpa, S.K. Sarkar and T. Mukherjee, Journal of Molecular Catalysis A: Chemical, 318, 106 (2010).
31. S. Buddee, S. Wongnawa, P. Sriprang and C. Sriwong, Journal of Nanoparticle Research, 16, 2336 (2014).
32. P. Hohenberg and W. Kohn, Phys. Rev., 136, B864 (1964).
33. W. Kohn and L. Sham, Phys. Rev., 140, A1133 (1965).
34. The code, OPENMX, pseudoatomic basis functions, and pseudopotentials are available on a web site 'http://www.openmxsquare.org'.
35. T. Ozaki and H. Kino, Numerical atomic basis orbitals from H to Kr, Phys. Rev. B., 195113 69 (2004).
36. J.P. Perdew and A. Zunger, Phys. Rev. B., 23, 5048 (1981).
37. A. Koklj, Comput. Mater. Sci., 28, 155 (2003).
38. S. Grimme, J. Comput. Chem., 27(15), 1787 (2006).
39. The data available at 'http://rruff.geo.arizona.edu/AMS/amcsd.php'.
40. R.W.G. Wyckoff. Crystal structures, Second edition. Interscience Publishers, USA, New York, (1963).
41. Y. Lei, H. Liu and W. Xiao, J. Modelling Simul. Mater. Sci. Eng., 18, 025004 (2010).
42. A. Abbasi, J. J. Sardroodi and A. R. Ebrahimzadeh, Surf. Sci., 654, 20 (2016).